Magnetic oscillations of in-plane conductivity in quasi-two-dimensional metals

T. I. Mogilyuk
National Research Centre "Kurchatov Institute," Moscow 123182, Russia

P. D. Grigoriev*
L. D. Landau Institute for Theoretical Physics, Chernogolovka 142432, Russia
and National University of Science and Technology "MISiS," Moscow 119049, Russia

(Received 19 February 2018; revised manuscript received 13 June 2018; published 13 July 2018)

We develop the theory of transverse magnetoresistance in layered quasi-two-dimensional (Q2D) metals. Using the Kubo formula and harmonic expansion, we calculate intralayer conductivity in a magnetic field perpendicular to conducting layers. The analytical expressions for the amplitudes and phases of magnetic quantum oscillations (MQO) and of the so-called slow oscillations (SO) are derived and applied to analyze their behavior as a function of several parameters: magnetic field strength, interlayer transfer integral, and Landau-level width. Both the MQO and SO of intralayer and interlayer conductivities have approximately opposite phase in weak magnetic field and the same phase in strong field. The amplitude of SO of intralayer conductivity changes sign at $\omega_c\tau_0 = \sqrt{3}$. There are several other qualitative differences between magnetic oscillations of in-plane and out-of-plane conductivity. The results obtained are useful to analyze experimental data on magnetoresistance oscillations in various strongly anisotropic Q2D metals.

DOI: 10.1103/PhysRevB.98.045118

I. INTRODUCTION

Magnetic quantum oscillations (MQO) are powerful tools for studying electronic dispersion and Fermi-surface (FS) geometry of metallic compounds [1–3]. In recent decades it has been actively used to investigate the electronic structure of strongly anisotropic layered compounds, including organic metals (see, e.g., Refs. [4–9] for reviews), high-temperature superconductors [10–19] (reviewed in Refs. [20–22]), etc. In layered compounds magnetoresistance (MR) has several new and useful qualitative effects, which do not appear in almost isotropic three-dimensional (3D) metals. The theory of magnetoresistance in two-dimensional (2D) metals [23,24], extensively developed in connection to quantum Hall effect, is also inapplicable to quasi-2D (Q2D) metals; even a weak interlayer hopping changes drastically the 2D localization effects and most electronic properties.

The FS of layered metals, e.g., corresponding to the electron dispersion in Eq. (3), is a warped cylinder. Such a FS has two close extremal cross-section areas S_1 and S_2 by the planes in k space perpendicular to magnetic field $\boldsymbol{B}$, which give two close MQO frequencies $F_{1,2} = S_{1,2}/(2\pi e\hbar)$. According to the standard theory [1–3], the observed MQO are given by the sum of oscillations with these two frequencies and almost equal amplitudes, which gives the beats of MQO amplitude [3], typical to Q2D metals. The beat frequency

$$\Delta F \equiv F_1 - F_2 \approx 2t_z B_z/(\hbar\omega_c) \tag{1}$$

can be used to measure the interlayer transfer integral $t_z \approx \Delta F\hbar\omega_c/(2B_z)$, while its nontrivial dependence on the tilt angle θ of magnetic field (with respect to the normal to conducting layers), given by [25]

$$\Delta F(\theta)/\Delta F(0) = J_0(k_F d\tan\theta), \tag{2}$$

allows one to extract the in-plane Fermi momentum k_F. As follows from Eq. (2), the beat frequency $\Delta F(\theta)$ goes to zero in the so-called Yamaji angles θ_{Yam}, given by the zeros of the Bessel function: $J_0(k_F d\tan\theta_{\mathrm{Yam}}) = 0$. The angular oscillations of the effective interlayer transfer integral $t_z(\theta)$, given by Eq. (2), also result in the angular magnetoresistance oscillations (AMRO), first discovered [26] in Q2D organic metal β-(BEDT-TTF)$_2$IBr$_2$ in 1988 and then actively studied both in Q2D and quasi-one-dimensional organic metals [4–9,27–30]. The interplay between AMRO and MQO is also nontrivial [30,31] and leads to some new effects, such as "false spin zeros" [31].

Another interesting feature of magnetoresistance in Q2D metals is the so-called slow oscillations (SO) [32,33]. These oscillations come from the mixing of two close frequencies F_1 and F_2 and have the frequency equal to the doubled beat frequency in Eq. (1). Similarly to AMRO and contrary to the usual MQO, the SO are not sensitive to the smearing of the Fermi level, because they contain only the difference of Fermi levels at different k_z given by t_z. Hence, the SO are usually much stronger than the true MQO and can be observed at much higher temperature [32,34]. These slow oscillations were first observed in layered organic metal β-(BEDT-TTF)$_2$IBr$_2$ and erroneously interpreted as MQO from small FS pockets [26,35]. Similar oscillations have also been observed in other organic conductors, e.g., β-(BEDT-TTF)$_2$I$_3$ [36,37], κ-(BEDT-TTF)$_2$Cu$_2$(CN)$_3$ [38], and κ-(BEDT-TSF)$_2$C(CN)$_3$ [39], while the band-structure calculations [6] do not predict the corresponding small FS pockets in these compounds. The

*Corresponding author: grigorev@itp.ac.ru

k_z dispersion is not the only possible source of SO. In fact, any splitting of the electron dispersion, leading to two close FS extremal cross-section areas, produces slow oscillations of MR with frequency given by the double difference between these FS areas. For example, the bilayer crystal structure, common in many cuprate high-T_c superconductors and in numerous other strongly anisotropic materials, produces such splitting of the electron spectrum and the corresponding SO [34,40,41].

The SO turn out to be quite useful to study the parameters of electronic structure of layered metals. First, their frequency $F_{SO} = 2\Delta F$ gives the difference between the two close extremal FS cross-section areas. Depending on the origin of SO, this gives the strength of FS warping due to k_z dispersion and the value of the interlayer transfer integral t_z according to Eq. (1), the bilayer splitting, or another type of splitting of the electron spectrum. Second, the Dingle temperature T_D^* of SO is considerably less than the Dingle temperature T_D of MQO [32], because at low temperature it only contains the contribution from short-range impurities and does not contain the variations of the Fermi level due to long-range spatial inhomogeneities that damp MQO. Hence, the comparison of the Dingle temperatures of SO and MQO gives information about the type of disorder. In typical samples of organic metal β-(BEDT-TTF)$_2$I$_3$ the ratio $T_D/T_D^* \approx 5.3 \gg 1$ [32], which makes SO much stronger than MQO at any temperature. Third, if SO are due to k_z dispersion, the angular dependence of SO frequency gives the in-plane Fermi momentum k_F according to Eq. (2).

In addition to SO, in Q2D metals there is another notable effect of a phase shift of the beats of MQO of interlayer conductivity as compared to magnetization [42]. This phase shift increases with the increase of magnetic field. The explanation and calculation of this effect [33,42], done using the Boltzmann transport equation and the Kubo formula, have shown that, similarly to SO, it appears when the terms $\sim\hbar\omega_c/t_z$ are not neglected. Hence, in almost isotropic 3D metals, where t_z is of the order of Fermi energy $E_F \gg \hbar\omega_c$, both effects are negligibly small. However, in Q2D conductors, where $\hbar\omega_c/t_z \sim 1$, both effects can be strong.

The rigorous theory of SO was developed only for the interlayer magnetoresistance [32,33]. However, their quite generic origin and various experiments [12,19,34] suggest that similar SO must also be observed in the in-plane electronic transport. A semiphenomenological description of in-plane SO, proposed in Refs. [34,41], does not contain the calculation of in-plane diffusion coefficient $D_{||}$ but only assumes that its oscillations have the same phase as the oscillations of the density of states (DOS) due to the Landau quantization. Even this is not generally valid, as we show below. In addition, in Refs. [34,41,43] the amplitude of MQO of $D_{||}$, which affects the amplitude and even the sign of SO of intralayer MR, has not been calculated.

In this paper we calculate the in-plane MR in layered Q2D metals using the Feynman diagram technique. This calculation shows some qualitative differences of intralayer and interlayer MR. For example, the amplitude of SO turns out to have nonmonotonic magnetic field dependence and may even change the sign. The phase shifts of MQO and their beats in Q2D metals also differ for intralayer and interlayer MR.

II. THE MODEL AND BASIC FORMULAS

Let us consider layered Q2D metals with electron dispersion

$$\epsilon_{3D}(\boldsymbol{k}) = \hbar^2\left(k_x^2 + k_y^2\right)/(2m_*) - 2t_z\cos(k_z d), \tag{3}$$

where the interlayer transfer integral t_z is assumed to be independent of electron momentum [44]. In a magnetic field $\boldsymbol{B}$ along the z axis, i.e., perpendicular to conducting layers, its electron dispersion becomes

$$\epsilon(n, k_z) = \hbar\omega_c\left(n + \tfrac{1}{2}\right) - 2t_z\cos(k_z d), \tag{4}$$

where $\omega_c = eB_z/(m_* c)$ is cyclotron frequency, m_* is effective electron mass, e is the electric charge, and c is the speed of light. The diagonal component of the in-plane conductivity tensor $\sigma_{ij}(\varepsilon)$ is given by [28,48–51]

$$\sigma_{xx}(\varepsilon) = \frac{e^2\hbar}{\pi V}\sum_{\{n,\,n'\}=0}^{+\infty}\sum_{k_x,\,k_z}|\langle n', k_x, k_z|v_x|k_z, k_x, n\rangle|^2 \times \mathrm{Im}G_{n'}^R(k_x, k_z, \varepsilon)\mathrm{Im}G_n^R(k_x, k_z, \varepsilon), \tag{5}$$

where $V = L_x L_y L_z$ is the volume, which is canceled after the summation over momenta, $\mathrm{Im}G_n^R$ represents the imaginary part of the retarded electron Green's function G_n^R, and v_x is the electron velocity along x axis. The matrix elements $\langle n', k_x, k_z|v_x|k_z, k_x, n\rangle$ of electron velocity $v_x = p_x/m_*$ in the basis of the Landau-gauge quantum numbers $\{k_x, k_z, n\}$ of an electron in magnetic field are given by [28]

$$\langle n', k_x, k_z|v_x|k_z, k_x, n\rangle = \frac{-i\hbar}{\sqrt{2}m_* l_H}\left(\sqrt{n'+1}\,\delta_{n,n'+1} - \sqrt{n'}\,\delta_{n,n'-1}\right), \tag{6}$$

where $l_H = \sqrt{\hbar c/(eB_z)} = \sqrt{\hbar/(m_*\omega_c)}$ is the magnetic length. Equation (6) can be checked by a direct calculation. The square of this matrix element of electron velocity is

$$|\langle n-1, k_x, k_z|v_x|k_z, k_x, n\rangle|^2 = \frac{\hbar^2 n}{2m_*^2 l_H^2}. \tag{7}$$

The summation over momenta in Eq. (5) can be replaced by the integration according to

$$\sum_{k_x} = \int_0^{L_y/l_H^2}\frac{dk_x L_x}{2\pi}, \quad \sum_{k_z} = \int_{-\pi/d}^{\pi/d}\frac{dk_z L_z}{2\pi}. \tag{8}$$

In the Born approximation or even in the self-consistent Born approximation (SCBA) the self-energy part $\Sigma^R(\varepsilon)$ from short-range impurity scattering depends only on electron energy ε and does not depend on electron quantum numbers [33,52–55], and the electron Green's function does not depend on k_x:

$$\mathrm{Im}G_n^R(k_x, k_z, \varepsilon) = \mathrm{Im}G_n^R(k_z, \varepsilon) = \frac{\mathrm{Im}\Sigma^R(\varepsilon)}{[\varepsilon - \epsilon_n + 2t_z\cos(k_z d) - \mathrm{Re}\Sigma^R(\varepsilon)]^2 + [\mathrm{Im}\Sigma^R(\varepsilon)]^2}, \tag{9}$$

where $\epsilon_n = \hbar\omega_c(n + 1/2)$. Substituting Eqs. (7)–(9) in Eq. (5) one obtains the expression for diagonal conductivity in the

SCBA approximation:

$$\sigma_{xx}(\varepsilon) = \frac{e^2(\hbar\omega_c)^2\Gamma^2}{4\pi^3\hbar}\int_{-\pi/d}^{\pi/d} dk_z \times \sum_{n=0}^{+\infty} \frac{n\{[\epsilon_{n+1} - \varepsilon_* - 2t_z\cos(k_z d)]^2 + \Gamma^2\}^{-1}}{[\epsilon_n - \varepsilon_* - 2t_z\cos(k_z d)]^2 + \Gamma^2}, \tag{10}$$

where we introduced the notations

$$\varepsilon_* \equiv \varepsilon - \mathrm{Re}\Sigma^R(\varepsilon), \quad \Gamma \equiv |\mathrm{Im}\Sigma^R(\varepsilon)|. \tag{11}$$

Introducing the dimensionless quantities

$$\alpha \equiv \alpha(\varepsilon_*) \equiv 2\pi\varepsilon_*/(\hbar\omega_c),\ a \equiv \alpha(\varepsilon_*) + \lambda\cos(k_z d), \tag{12}$$

$$\lambda = 4\pi t_z/(\hbar\omega_c),\ \gamma = 2\pi\Gamma/(\hbar\omega_c), \tag{13}$$

we can rewrite the expression (10) for diagonal conductivity as

$$\sigma_{xx}(\varepsilon) = \frac{e^2\gamma^2}{\pi\hbar}\int_{-\pi/d}^{\pi/d} dk_z \sum_{n=0}^{+\infty} f(n), \tag{14}$$

where

$$f(n) \equiv \frac{n\{[2\pi(n-\frac{1}{2}) - a]^2 + \gamma^2\}^{-1}}{[2\pi(n+\frac{1}{2}) - a]^2 + \gamma^2}. \tag{15}$$

III. HARMONIC EXPANSION OF CONDUCTIVITY

The sum over the Landau-level (LL) index n in Eq. (14) can be transformed to the sum over harmonics using the Poisson summation formula [56], given by

$$\sum_{n=0}^{+\infty} f(n) = \sum_{p=-\infty}^{+\infty}\int_h^{+\infty} dn f(n)\exp(2\pi i p n), \tag{16}$$

where the number $h \in (-1, 0)$. In the limit of strong harmonic damping, i.e., when the factor $R_D J_0(\lambda) \ll 1$, where $R_D = \exp(-\gamma) \approx R_{D0} = \exp(-\gamma_0) = \exp[-2\pi^2 k_B T_D/(\hbar\omega_c)]$ is the Dingle factor, we may keep only the zeroth and first harmonics in this expansion:

$$\sigma_{xx}(\varepsilon) \approx \sigma_{xx}^{(0)}(\varepsilon) + \sigma_{xx}^{(1)}(\varepsilon), \tag{17}$$

where the zeroth-harmonic term

$$\sigma_{xx}^{(0)}(\varepsilon) = \frac{e^2\gamma^2}{\pi\hbar}\int_{-\pi/d}^{\pi/d} dk_z \int_{-1/2}^{+\infty} dn f(n), \tag{18}$$

and the first-harmonic term

$$\sigma_{xx}^{(1)}(\varepsilon) = 2\frac{e^2\gamma^2}{\pi\hbar}\int_{-\pi/d}^{\pi/d} dk_z \int_{-1/2}^{+\infty} dn f(n)\cos(2\pi n). \tag{19}$$

The integrals in Eqs. (18) and (19) simplify in the limit when the number n_F of filled LLs is large, i.e., when $a \sim E_F/(\hbar\omega_c) \approx n_F \gg 1$, where E_F is the Fermi energy. Then, after changing the integration variable from n to $l = 2\pi(n + 1/2) - a$, we can also change the lower integration limit from $-a$ to $-\infty$, because all integrals converge at a lower integration limit. The integral over n in Eq. (18) becomes

$$\int_{-1/2}^{+\infty} dn f(n) \approx \int_{-\infty}^{+\infty} \frac{dl(l + a - \pi)/(2\pi)^2}{(l^2 + \gamma^2)[(l-1)^2 + \gamma^2]} = \frac{a}{8\pi\gamma(\gamma^2 + \pi^2)}, \tag{20}$$

and substituting this in Eq. (18) we obtain

$$\sigma_{xx}^{(0)}(\varepsilon) = \frac{e^2\gamma}{8\pi^2\hbar}\int_{-\pi/d}^{\pi/d} dk_z \frac{\lambda\cos(k_z d) + \alpha}{\gamma^2 + \pi^2} = \frac{e^2}{4\pi\hbar d}\frac{\alpha\gamma}{\gamma^2 + \pi^2}. \tag{21}$$

Similarly, at $a \gg 1$ the integration over n in expression (19) for $\sigma_{xx}^{(1)}(\varepsilon)$ gives

$$\int_{-1/2}^{+\infty} dn f(n)\cos(2\pi n) \approx \frac{a\gamma\cos(a)}{8\pi(\gamma^2 + \pi^2)}\exp(-\gamma). \tag{22}$$

Substituting this and Eq. (12) in Eq. (19), we obtain the integral over k_z only, which can be easily taken as

$$\sigma_{xx}^{(1)}(\varepsilon) = -\frac{e^2\gamma}{4\pi^2\hbar}\int_{-\pi/d}^{\pi/d} dk_z \frac{\alpha(\varepsilon_*) + \lambda\cos(k_z d)}{\gamma^2 + \pi^2} \times \cos[\alpha(\varepsilon_*) + \lambda\cos(k_z d)]\exp(-\gamma) = -\frac{e^2\alpha}{2\pi\hbar d}\frac{\gamma\exp(-\gamma)}{\gamma^2 + \pi^2}\left[J_0(\lambda)\cos(\alpha) - \frac{\lambda}{\alpha}J_1(\lambda)\sin(\alpha)\right], \tag{23}$$

where to integrate over k_z we used the identities [57,58]

$$\int_{-\pi}^{\pi} dn \exp[ia\cos(n)] = 2\pi J_0(a), \tag{24}$$

$$\int_{-\pi}^{\pi} dn \cos(n)\exp[ia\cos(n)] = 2\pi i J_1(a). \tag{25}$$

If $\lambda/\alpha \approx 2t_z/E_F \ll 1$, in Eq. (23) one can neglect the last term in the square brackets, but at $2t_z/E_F \sim 1$ it must be kept. This term gives the phase shift of MQO of conductivity and leads to the finite amplitude of MQO even in the beat nodes [see Eq. (41) below], which can be used to measure the ratio $2t_z/E_F$.

In the SCBA for pointlike impurity scattering the electron self-energy is proportional to the Green's function in the coinciding points $G(r, r, \varepsilon)$, and its oscillations are given by [33]

$$\frac{\Sigma^R(\varepsilon)}{\Gamma_0} = A(\varepsilon) - i - 2i\sum_{p=1}^{+\infty}(-1)^p \exp\{p[i\alpha(\varepsilon_*) - \gamma]\}J_0(\lambda p), \tag{26}$$

where Γ_0 is a nonoscillating part of $\mathrm{Im}\,\Sigma^R(\varepsilon)$, related to mean free time $\tau_0 = \hbar/(2\Gamma_0)$ without magnetic field, and $A(\varepsilon)$ is a slowly varying function of energy ε, which only shifts the chemical potential. Hence, $A(\varepsilon)$ does not affect the observed conductivity and is hereinafter neglected.

Below we find explicitly all the terms which contribute to MQO and SO in the lowest order in the small factor $R_D J_0(\lambda)$.

A. Contribution from the zeroth-harmonic term $\sigma_{xx}^{(0)}$

Equation (21) is an oscillating function of ε, because it contains oscillating functions $\gamma(\varepsilon)$ and $\alpha(\varepsilon_*)$. Keeping only zeroth and first harmonics in Eq. (26) we obtain

$$\gamma = \gamma(\varepsilon) \approx \gamma_0[1 - 2\exp(-\gamma)\cos(\alpha)J_0(\lambda)], \tag{27}$$

and $\alpha = \alpha(\varepsilon_*)$ also contains oscillations coming from $\mathrm{Re}\Sigma^R(\varepsilon)$ in Eq. (26). However, the relative amplitude of $\alpha(\varepsilon_*)$ oscillations is much smaller, namely, by a factor $\gamma_0/\alpha \approx \Gamma_0/E_F \ll 1$, than that of $\gamma(\varepsilon)$, although their absolute amplitudes are comparable. Hence, in Eq. (21) the oscillations of $\alpha(\varepsilon_*)$ can be neglected. Note that the products $\cos(\alpha)e^{-\gamma}$ and $\sin(\alpha)e^{-\gamma}$ do not give the SO in the second order in R_D. Indeed, using Eq. (26) and introducing the small parameter

$$\gamma_1 \equiv 2\gamma_0 R_D J_0(\lambda) \ll 1, \tag{28}$$

in the second order in R_D we obtain

$$\cos(\alpha) \approx \cos[\overline{\alpha} + \gamma_1\sin(\overline{\alpha})] \approx \cos[\overline{\alpha}] - \gamma_1\sin^2(\overline{\alpha}), \tag{29}$$

where $\overline{\alpha} = 2\pi\overline{\varepsilon}_*/(\hbar\omega_c) = 2\pi E_F/(\hbar\omega_c)$ is the value of α averaged over the MQO period, and

$$\exp(-\gamma) \approx R_D\exp[\gamma_1\cos(\overline{\alpha})] \approx R_D[1 + \gamma_1\cos(\overline{\alpha})]. \tag{30}$$

In the second order in R_D the product

$$\begin{aligned}\cos(\alpha)\exp(-\gamma) &\approx R_D\{\cos[\overline{\alpha}] + \gamma_1[\cos^2(\overline{\alpha}) - \sin^2(\overline{\alpha})]\}\\ &= R_D(\cos[\overline{\alpha}] + \gamma_1\cos[2\overline{\alpha}])\end{aligned} \tag{31}$$

does not contain the constant term giving SO but only the second harmonics $\cos[2\overline{\alpha}]$. Similarly,

$$\sin(\alpha) \approx \sin[\overline{\alpha} + \gamma_1\sin(\overline{\alpha})] \approx \sin[\overline{\alpha}] + \gamma_1\cos(\overline{\alpha})\sin(\overline{\alpha}) \tag{32}$$

and $\sin(\alpha)\exp(-\gamma)$ do not contain constant or SO terms in the second order in $R_D J_0(\lambda)$. Hence, in the second order in R_D, Eq. (27) simplifies to

$$\gamma \approx \gamma_0[1 - 2\exp(-\gamma_0)J_0(\lambda)\cos(\overline{\alpha})]. \tag{33}$$

Substituting Eq. (33) in Eq. (21), expanding up to the second order in $R_D J_0(\lambda)$, and replacing α with $\overline{\alpha}$ we obtain [59]

$$\sigma_{xx}^{(0)}(\varepsilon) = \overline{\sigma}_{xx}^{(0)}(\varepsilon) + \sigma_{xx}^{(0)}(\varepsilon)_{\mathrm{QO}} + \sigma_{xx}^{(0)}(\varepsilon)_{\mathrm{SO}}, \tag{34}$$

where the nonoscillating Drude conductivity

$$\overline{\sigma}_{xx}^{(0)}(\varepsilon) = \overline{\sigma}_{xx}^{(0)} \approx \frac{e^2}{4\pi\hbar d}\frac{\overline{\alpha}\gamma_0}{\gamma_0^2 + \pi^2}, \tag{35}$$

the fast quantum oscillations of conductivity come from the first-order term in $R_D J_0(\lambda)$ and are given by

$$\sigma_{xx}^{(0)}(\varepsilon)_{\mathrm{QO}} \approx 2\overline{\sigma}_{xx}^{(0)} R_D J_0(\lambda)\frac{\gamma_0^2 - \pi^2}{\gamma_0^2 + \pi^2}\cos(\overline{\alpha}), \tag{36}$$

and the slow oscillations of conductivity appear in the second order in $R_D J_0(\lambda)$:

$$\sigma_{xx}^{(0)}(\varepsilon)_{\mathrm{SO}} \approx 2\overline{\sigma}_{xx}^{(0)}\frac{\gamma_0^2(\gamma_0^2 - 3\pi^2)}{(\gamma_0^2 + \pi^2)^2}R_D^2 J_0^2(\lambda), \tag{37}$$

where we have used the identity $\cos^2(\overline{\alpha}) = [1 + \cos(2\overline{\alpha})]/2$ and neglected the second harmonics of MQO, i.e., omitted terms $\propto \cos(2\overline{\alpha})$.

B. Contribution from the first-harmonic term $\sigma_{xx}^{(1)}$ and total expressions for magnetic oscillations

To find the fast quantum oscillations of $\sigma_{xx}^{(1)}(\varepsilon)$ in the lowest order in $R_D J_0(\lambda)$ it is sufficient to replace γ by γ_0 and $\alpha(\varepsilon_*)$ by its average value $\overline{\alpha}$ in Eq. (23):

$$\sigma_{xx}^{(1)}(\varepsilon)_{\mathrm{QO}} \approx -2\overline{\sigma}_{xx}^{(0)} R_D\left[J_0(\lambda)\cos(\overline{\alpha}) - \frac{\lambda}{\overline{\alpha}}J_1(\lambda)\sin(\overline{\alpha})\right]. \tag{38}$$

Then, the sum of Eqs. (36) and (38) gives the total fast quantum oscillations in the first order in $R_D J_0(\lambda)$:

$$\begin{aligned}\sigma_{xx}^{\mathrm{QO}}(\varepsilon) &= \sigma_{xx}^{(0)}(\varepsilon)_{\mathrm{QO}} + \sigma_{xx}^{(1)}(\varepsilon)_{\mathrm{QO}}\\ &\approx -2\overline{\sigma}_{xx}^{(0)} R_D\left[\frac{2\pi^2 J_0(\lambda)}{\gamma_0^2 + \pi^2}\cos(\overline{\alpha}) - \frac{\lambda}{\overline{\alpha}}J_1(\lambda)\sin(\overline{\alpha})\right].\end{aligned} \tag{39}$$

We transform this trigonometric expression to

$$\sigma_{xx}^{\mathrm{QO}}(\varepsilon) \approx -A_{xx}^{\mathrm{QO}}\cos(\overline{\alpha} + \Delta\phi_{\mathrm{QO}}), \tag{40}$$

where the amplitude of MQO is given by

$$A_{xx}^{\mathrm{QO}} = 2\overline{\sigma}_{xx}^{(0)} R_D\sqrt{\frac{4\pi^4}{(\gamma_0^2 + \pi^2)^2}J_0^2(\lambda) + \left(\frac{\lambda}{\overline{\alpha}}\right)^2 J_1^2(\lambda)} \tag{41}$$

and a phase shift of MQO is

$$\Delta\phi_{\mathrm{QO}} = \arccos\left[\frac{2\pi^2 J_0(\lambda)\overline{\alpha}}{\sqrt{[2\pi^2 J_0(\lambda)\overline{\alpha}]^2 + [\lambda J_1(\lambda)(\gamma_0^2 + \pi^2)]^2}}\right]. \tag{42}$$

This phase shift jumps by $\sim\pi$ and changes the sign of $\sigma_{xx}^{\mathrm{QO}}$ at certain values of magnetic field, corresponding to the beats of MQO at $J_0(\lambda) = 0$. The second term in the denominator makes this phase jump smoother and is missing in phenomenological theories [34,41].

The derived expressions (39)–(42), describing the MQO of in-plane conductivity in the lowest nonvanishing order in $R_D J_0(\lambda)$, have several important features. Due to the second term in Eq. (39), the MQO amplitude A_{xx}^{QO}, given by Eq. (41) and plotted in Fig. 1, is nonzero even at beat nodes $J_0(\lambda) = 0$, corresponding to the minima of MQO amplitude, where it increases with the increase of ratio $\lambda/\overline{\alpha} = 2t_z/E_F$. At maxima the MQO amplitude A_{xx}^{QO} is proportional to the square of electron velocity and, for a parabolic in-plane electron dispersion, to the Fermi energy E_F, in agreement with the standard theory [3] [see Fig. 1(a)]. Equations (39) and (41) suggest that at $\gamma_0 \gtrsim \pi$, in addition to the standard Dingle factor, the MQO are damped by the factor $1/(\gamma_0^2 + \pi^2)$. We illustrate all this in Fig. 1 by plotting the amplitude A_{xx}^{QO} as a function of $1/\lambda = B_z/(2\pi\Delta F)$ for three different ratios of t_z/E_F. In Fig. 1(a) we keep t_z fixed and vary E_F, which may correspond to different Fermi-surface pockets or Fermi-surface reconstruction, and in Fig. 1(b) we keep E_F fixed and vary t_z. In all figures the MQO amplitude increases with the increase of magnetic field because of the Dingle factor. In Fig. 1(a) at the beat nodes the MQO amplitude is the same for all three curves because E_F^{-1} in the factor t_z/E_F is compensated by the overall factor

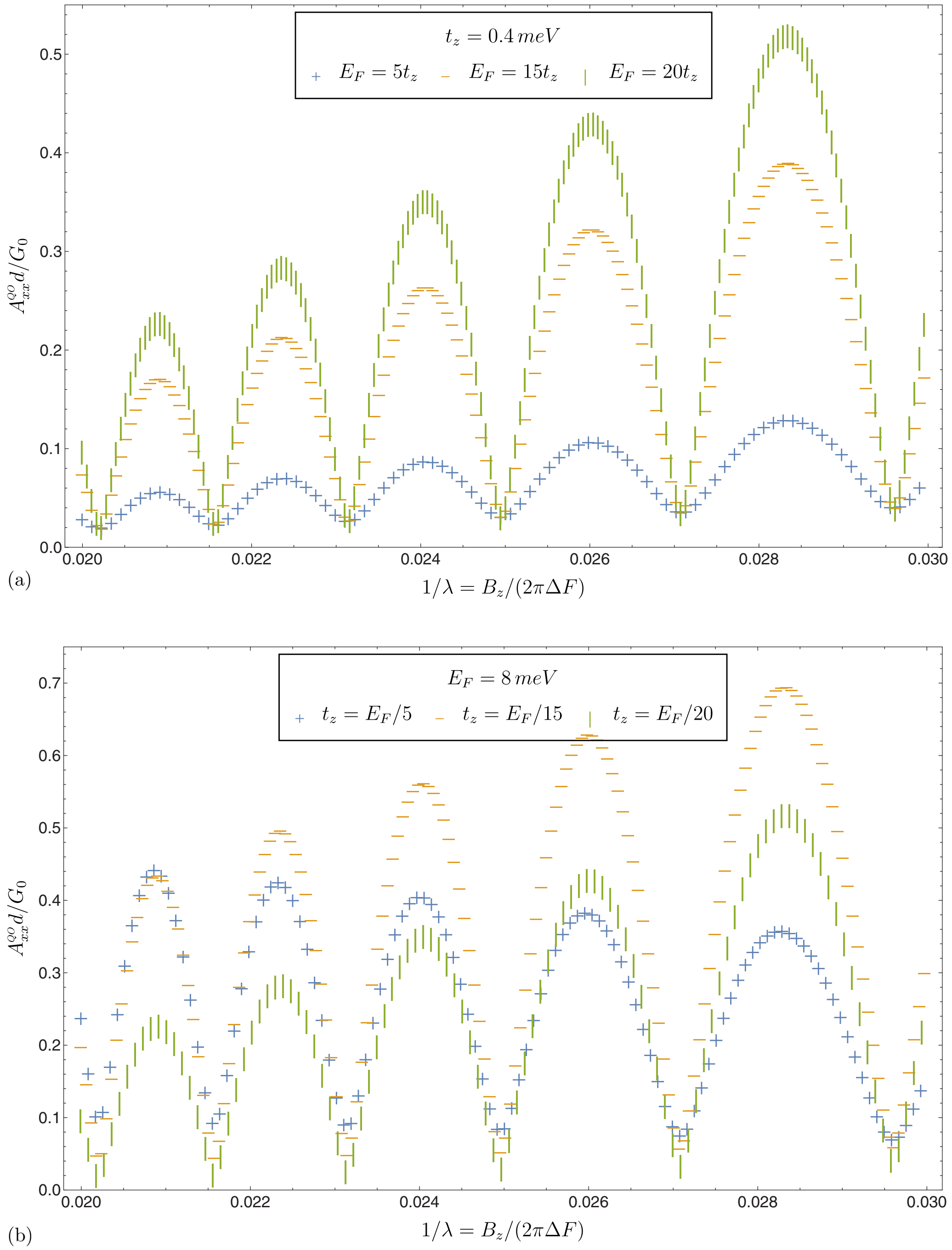

FIG. 1. The amplitude of quantum oscillations of in-plane diagonal conductivity for three different ratios t_z/E_F. (a) The amplitude of quantum oscillations of normalized in-plane diagonal conductivity $A_{xx}^{\mathrm{QO}} d/G_0$ given by Eq. (41) as a function of $1/\lambda \sim B_z$ [here $G_0 = e^2/(\pi\hbar)$ is the quantum of conductance] for three different values of Fermi energy E_F. The positions of local minima of MQO amplitude (beat nodes) do not depend on Fermi energy E_F, but the amplitude of MQO amplitude does according to Eq. (41) and discussion after Eq. (42). The taken parameters are $m_* = 0.04 m_e$, $\Gamma_0 = 14.5\, K$, $t_z = 10$ meV, $E_F = \{5, 10, 20\} t_z$. (b) The same as in panel (a) at fixed E_F but for three different values of t_z. The values at local minima of MQO depend on t_z. The taken parameters are $m_* = 0.04 m_e$, $\Gamma_0 = 14.5\, K$, $t_z = \{1/5, 1/15, 1/20\} E_F$, $E_F = 200$ meV.

E_F in $\overline{\sigma}_{xx}^{(0)}$. In Fig. 1(b) three different curves, corresponding to various values of t_z, also correspond to different magnetic field strength, because we plotted A_{xx}^{QO} as a function of $1/\lambda \propto B_z/t_z$. Therefore, at low field the blue curve, corresponding to $t_z = E_F/5$, is higher at MQO maxima. The second term in Eq. (39) also results in additional phase shift in Eq. (42), which depends on magnetic field via λ and γ_0 and is essential only near the beat nodes $J_0(\lambda) = 0$, as illustrated in Fig. 2.

To find the slow oscillations of $\sigma_{xx}^{(1)}(\varepsilon)$ in the lowest (second) order in $R_D J_0(\lambda)$ we need to expand γ in Eq. (23) according to Eq. (33) and take into account oscillations of α. This expansion

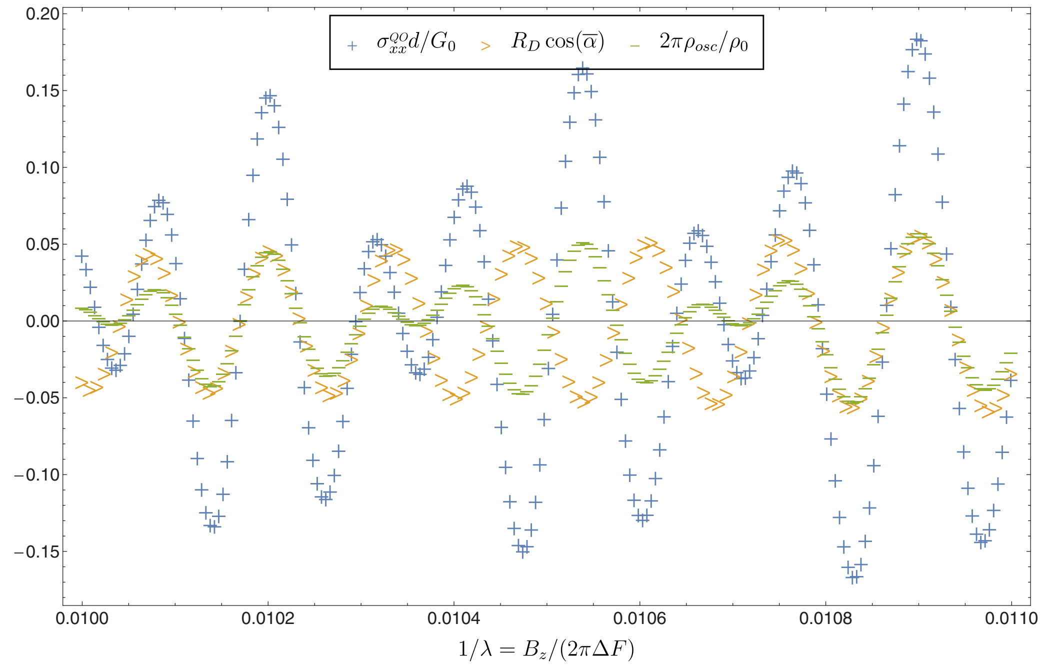

FIG. 2. Quantum oscillations of in-plane diagonal conductivity as compared to $R_D\cos(\overline{\alpha})$ and to the oscillating part $\rho_{\rm osc}$ of the DOS, where $\rho_{\rm osc} \equiv -2\rho_0\cos(\overline{\alpha})R_D J_0(\lambda)$. The phases of DOS and of σ_{xx} oscillations coincide everywhere except the proximity of beat nodes. The taken parameters are $m_* = 0.04m_e$, $\Gamma_0 = 14.5\,K$, $t_z = 20$ meV, $E_F = 200$ meV.

gives

$$\sigma_{xx}^{(1)}(\varepsilon) - \sigma_{xx}^{(1)}(\varepsilon)_{\rm QO} \approx 4\overline{\sigma}_{xx}^{(0)}\frac{\pi^2-\gamma_0^2}{\gamma_0^2+\pi^2}R_D^2 J_0(\lambda) \times \cos(\overline{\alpha})\left[J_0(\lambda)\cos(\overline{\alpha}) - \frac{\lambda}{\overline{\alpha}}J_1(\lambda)\sin(\overline{\alpha})\right], \tag{43}$$

and the SO coming from this expression are given by

$$\sigma_{xx}^{(1)}(\varepsilon)_{\rm SO} \approx 2\overline{\sigma}_{xx}^{(0)}(\varepsilon)\frac{\pi^2-\gamma_0^2}{\gamma_0^2+\pi^2}R_D^2 J_0^2(\lambda). \tag{44}$$

The total SO of diagonal in-plane conductivity are given by the sum of Eqs. (37) and (44):

$$\sigma_{xx}^{\rm SO}(\varepsilon) \approx 2\pi^2\overline{\sigma}_{xx}^{(0)}R_D^2 J_0^2(\lambda)\frac{\pi^2-3\gamma_0^2}{(\gamma_0^2+\pi^2)^2}. \tag{45}$$

To summarize the calculations, the harmonic expansion [by the parameter $\gamma_1 \equiv 2\gamma_0 R_D J_0(\lambda) \ll 1$] of intralayer conductivity $\sigma_{xx}(\varepsilon)$ is given by the sum of three main terms:

$$\sigma_{xx}(\varepsilon) \approx \overline{\sigma}_{xx}^{(0)}(\varepsilon) + \sigma_{xx}^{\rm QO}(\varepsilon) + \sigma_{xx}^{\rm SO}(\varepsilon), \tag{46}$$

where the term $\overline{\sigma}_{xx}^{(0)}(\varepsilon)$ corresponds to the nonoscillating part of conductivity and is given by Eq. (35), $\sigma_{xx}^{\rm QO}(\varepsilon)$ describes the MQO of intralayer conductivity given by Eq. (39), and $\sigma_{xx}^{\rm SO}(\varepsilon)$ describes the slow oscillations of intralayer conductivity and is given by Eq. (45).

C. Damping by temperature and sample inhomogeneities

As was shown in Refs. [32,33,41], the smearing of the Fermi level by temperature and by long-range sample inhomogeneities damps only the fast MQO $\sigma_{xx}^{\rm QO}(\varepsilon)$, and does not affect the constant part $\overline{\sigma}_{xx}^{(0)}(\varepsilon)$ or the SO $\sigma_{xx}^{\rm SO}(\varepsilon)$. Indeed, at finite temperature T conductivity $\sigma_{xx} = \sigma_{xx}(T)$ is given by the integral of $\sigma_{xx}(\varepsilon)$ over electron energy ε weighted by the derivative of Fermi distribution function $n'_F(\varepsilon) = -1/\{4T\cosh^2[(\varepsilon-\mu)/(2T)]\}$ with the chemical potential $\mu = E_F$:

$$\sigma_{xx}(\mu, T) = \int d\varepsilon\,[-n'_F(\varepsilon)]\,\sigma(\varepsilon). \tag{47}$$

Among the three terms in Eq. (46) only the second term $\sigma_{xx}^{\rm QO}(\varepsilon)$, describing MQO, is a rapidly oscillating function of electron energy ε because of its dependence on $\overline{\alpha}(\varepsilon)$. As a result of the integration over ε, only this term acquires the additional temperature damping factor

$$R_T = [2\pi^2 k_B T/(\hbar\omega_c)]/\sinh[2\pi^2 k_B T/(\hbar\omega_c)], \tag{48}$$

and the electron energy ε is replaced by the chemical potential μ. The macroscopic spatial inhomogeneities smear the Fermi energy along the whole sample. Hence, in addition to the temperature smearing in Eq. (47), given by the integration over electron energy ε, conductivity σ acquires the coordinate smearing, given by the integration over Fermi energy μ around its average value μ_0 weighted by a normalized distribution function $D(\mu) = D_0[(\mu-\mu_0)/W]$ of width W: $\sigma = \int d\mu\,\sigma(\mu)D(\mu)$. Again, only the second term $\sigma_{xx}^{\rm QO}$, describing MQO, is a rapidly oscillating function of μ via $\overline{\alpha}(\mu)$, and only this term acquires additional damping factor

$$R_W = \int dx\,D_0(x)\cos[2\pi x W/(\hbar\omega_c)] = R_W[W/(\hbar\omega_c)], \tag{49}$$

due to the sample inhomogeneities. This damping of MQO by long-range sample inhomogeneities in layered organic metal β-(BEDT-TTF)$_2$IBr$_2$ was shown to be much stronger than the damping by usual short-range impurities [32], making the amplitude of SO much larger than that of MQO. The SO, given by Eq. (45), do not depend on μ and, hence, are not damped by the factor R_W. This property makes the observation of SO much easier than that of MQO. It was used in the alternative interpretation [40,41] of the observed [10–19] MQO in YBCO high-temperature superconductors.

D. Influence of electron spin on conductivity

All previous expressions are for spinless electrons. If we take into account the spin splitting of Fermi level $E_F \pm \frac{1}{2}g\mu_e|\boldsymbol{B}|$ (g is the electron g factor, and μ_e is the Bohr magneton) and sum expressions (35) for Drude conductivity over both spin components, we simply multiply the spinless result (35) by 2:

$$\overline{\sigma}_{xx}^{(0)}(\varepsilon) \approx \frac{e^2}{2\pi\hbar d}\frac{\overline{\alpha}\gamma_0}{\gamma_0^2+\pi^2}. \tag{50}$$

For MQO $\sigma_{xx}^{\mathrm{QO}}$, given by Eq. (39), the sum of both spin components gives

$$\sigma_{xx}^{\mathrm{QO}}(\varepsilon) \approx -2\overline{\sigma}_{xx}^{(0)}R_D R_S\left[\frac{2\pi^2 J_0(\lambda)}{\gamma_0^2+\pi^2}\cos(\overline{\alpha}) - \frac{\lambda}{\overline{\alpha}}J_1(\lambda)\sin(\overline{\alpha})\right], \tag{51}$$

where the spin damping factor R_S of MQO in quasi-2D metals with $t_z \ll E_F$ is $R_S = \cos[\pi g m_*/(2m_e\cos\theta)]$ (m_e is the free-electron mass).

The influence of spin splitting on SO depends on electron dispersion and on the coupling between two spin components. For the parabolic in-plane dispersion, given by Eq. (3), and in the absence of any coupling between two spin components, the Zeeman spin splitting only adds a factor of 2 to $\sigma_{xx}^{\mathrm{SO}}$, similar to the Drude term. Indeed, the SO term in Eq. (45) does not depend on energy, and the sum over two spin-split energy bands only adds a factor of 2 to the final expression. However, for a more complicated in-plane electron dispersion this simple conclusion may be violated. Moreover, in real compounds there is often some coupling between two spin components due to spin-dependent scattering, chemical-potential oscillations and oscillating magnetostriction, or other effects. This coupling between two spin components introduces additional terms to SO, which may lead to the angular dependence of SO amplitude and even to an analog of the spin-zero effect.

E. The limiting cases of large and small interlayer transfer integrals t_z

In this section we compare the results obtained with two previously known limiting cases, namely, 2D and 3D cases. The SO are specific to quasi-2D metals, being neglected in both these limiting cases. In the 2D case, $t_z = 0$, the SO have zero frequency and, hence, do not exist. In 3D metals, where $t_z \sim E_F \gg \hbar\omega_c$, the SO may exist but have too small amplitude, being less than MQO by a factor $\sim R_D\sqrt{\hbar\omega_c/(2\pi^2 t_z)} \ll 1$. Hence, below we compare only the usual MQO of intralayer conductivity.

In the 2D limiting case, taking $t_z = 0$ and $\lambda = 0$ in Eq. (39), we obtain the following expression for the MQO of intralayer conductivity:

$$\sigma_{xx}^{\mathrm{QO}}(\varepsilon, t_z = 0) \approx -\overline{\sigma}_{xx}^{(0)}R_D\frac{4\pi^2}{\gamma_0^2+\pi^2}\cos(\overline{\alpha}). \tag{52}$$

It coincides with Eq. (2.15) of Ref. [60], where the quantum transport in a 2D electron system under magnetic fields was studied. Note that the amplitude of MQO in Eq. (2.15) of Ref. [60] is twice larger than that in Eq. (2.16) of the same work [60] or in Eq. (6.40) of Ref. [23], where the quantum oscillations of $\mathrm{Im}\Sigma$ or τ are neglected.

The limiting 3D case corresponds to large $t_z \gg \hbar\omega_c$, i.e., $\lambda \gg 1$. In this limit one may use asymptotic expansions of the Bessel functions at large argument in Eq. (39): $J_0(\lambda) \approx \sqrt{2/(\pi\lambda)}\cos(\lambda - \pi/4)$, $J_1(\lambda) \approx \sqrt{2/(\pi\lambda)}\sin(\lambda - \pi/4)$. Then Eq. (39) simplifies to

$$\sigma_{xx}^{\mathrm{QO}}(\varepsilon) \approx -\left(\frac{2^3}{\pi\lambda}\right)^{1/2}\overline{\sigma}_{xx}^{(0)}R_D\left[\frac{2\pi^2\cos(\overline{\alpha})}{\gamma_0^2+\pi^2}\cos\left(\lambda-\frac{\pi}{4}\right) - \frac{\lambda}{\overline{\alpha}}\sin(\overline{\alpha})\sin\left(\lambda-\frac{\pi}{4}\right)\right]. \tag{53}$$

In a strong magnetic field $\gamma_0 \ll 1$, $R_D \approx 1$, and Eq. (53) in terms of initial parameters reduces to

$$\frac{\sigma_{xx}^{\mathrm{QO}}(\varepsilon)}{\overline{\sigma}_{xx}^{(0)}} \approx -\frac{2}{\pi}\left(\frac{2\hbar\omega_c}{t_z}\right)^{1/2} \times\left[\cos\left(\frac{2\pi E_F}{\hbar\omega_c}\right)\cos\left(\frac{4\pi t_z}{\hbar\omega_c}-\frac{\pi}{4}\right) - \frac{2t_z}{E_F}\sin\left(\frac{2\pi E_F}{\hbar\omega_c}\right)\sin\left(\frac{4\pi t_z}{\hbar\omega_c}-\frac{\pi}{4}\right)\right]. \tag{54}$$

We compare Eq. (54) with the expression obtained in Ref. [61] (see Eq. (4) of Ref. [61]) and written in a more convenient form in Eq. (90.22) of Ref. [62]:

$$(\sigma_{xx})_A = \sum_{\mathrm{ex}}\sum_{l=1}^{+\infty}(-1)^l\sigma_{xx}^{(l)}\cos\left\{l\frac{cS_{\mathrm{ex}}}{e\hbar B_z} \pm \frac{\pi}{4}\right\}, \tag{55}$$

where ex $\equiv$ {min, max} means the extremal cross section of the Fermi surface,

$$\sigma_{xx}^{(l)} = \frac{2^{5/2}\pi^{1/2}(e\hbar)^{1/2}b_{\mathrm{ex}}}{c^{1/2}B_z^{3/2}l^{1/2}}\left|\frac{\partial^2 S}{\hbar^2\partial k_z^2}\right|_{\mathrm{ex}}^{-1/2}, \tag{56}$$

and b_{ex} is the quantity $b_z(E_F, k_{z\,\mathrm{ex}}(E_F))$ given by Eqs. (90.13) and (90.15) of Ref. [62] and taken at points $k_{z\,ex}$, corresponding to Fermi-surface extremal cross sections. The "$\pm$" in Eq. (55) means "$-$" for maximum and "$+$" for minimum of the function $S_{\mathrm{ex}}(k_z)$ [63].

In our case there are two extremal cross sections over the period $2\pi/d$. These extremal cross-section areas of the Fermi surface are

$$S_{\mathrm{ex}} = 2\pi m_*[E_F + 2t_z\cos(k_z d)]|_{\mathrm{ex}} = 2\pi m_*(E_F \pm 2t_z). \tag{57}$$

Their second derivatives at extremal points are

$$\left.\frac{\partial^2 S}{\hbar^2\partial k_z^2}\right|_{\mathrm{ex}} = -\frac{4\pi m_* d^2 t_z}{\hbar^2}\cos(k_z d)\Big|_{\mathrm{ex}} = \mp\frac{4\pi m_* d^2 t_z}{\hbar^2}. \tag{58}$$

If we assume that $b_{\max} = b_{\min}$, which is valid at least if $t_z \ll E_F$, the sum over extremal cross sections for $l = 1$ in Eq. (55) can be simplified:

$$\sum_{\mathrm{ex}} \cos\left\{\frac{cS_{\mathrm{ex}}}{e\hbar B_z} \pm \frac{\pi}{4}\right\} = 2\cos\left(\frac{2\pi E_F}{\hbar\omega_c}\right)\cos\left(\frac{4\pi t_z}{\hbar\omega_c} - \frac{\pi}{4}\right). \tag{59}$$

Using auxiliary Eqs. (56), (58), and (59) in Eq. (55), we find the oscillating part of intralayer conductivity for the first harmonic $l = 1$:

$$\left(\sigma_{xx}^{\mathrm{QO}}\right)_A \approx -\sqrt{\frac{2^5 e\hbar^3 b_{\max}^2}{m_* c B_z^3 t_z d^2}}\cos\left(\frac{2\pi E_F}{\hbar\omega_c}\right)\cos\left(\frac{4\pi t_z}{\hbar\omega_c} - \frac{\pi}{4}\right). \tag{60}$$

From Eq. (90.15) on page 387 of Ref. [62] one can evaluate the intralayer conductivity σ_{xx} averaged over the period of magnetic oscillations:

$$(\overline{\sigma}_{xx})_A = \frac{2\hbar}{B_z^2}\int_{-\pi/d}^{\pi/d} b(E_F, k_z)dk_z \approx \frac{4\pi\hbar b_{\max}}{dB_z^2}. \tag{61}$$

Finally, gathering Eqs. (60) and (61), we find the ratio of oscillating and nonoscillating parts:

$$\frac{\left(\sigma_{xx}^{\mathrm{QO}}\right)_A}{(\overline{\sigma}_{xx})_A} \approx -\left(\frac{2\hbar\omega_c}{\pi^2 t_z}\right)^{1/2}\cos\left(\frac{2\pi E_F}{\hbar\omega_c}\right)\cos\left(\frac{4\pi t_z}{\hbar\omega_c} - \frac{\pi}{4}\right). \tag{62}$$

This is twice smaller than in Eq. (54), because in the derivation of Eqs. (55)–(62) the quantum oscillations of b_{ex} and, hence, of $\mathrm{Im}\Sigma$ are neglected. This extra factor of 2, arising from the oscillations of $\mathrm{Im}\Sigma$, is similar to that in the 2D case discussed above. If we neglected the MQO of $\mathrm{Im}\Sigma$, instead of Eq. (39) we would use Eq. (38). Then, performing similar expansion as in the derivation of Eqs. (53) and (54), from Eq. (38) we obtain Eq. (62) in the lowest order in t_z/E_F.

IV. DISCUSSION

The calculations of intralayer conductivity in the previous section shows that $\sigma_{xx}(\mu)$ can be divided into three parts:

$$\sigma_{xx}(\mu, T) \approx \overline{\sigma}_{xx}^{(0)}(\mu) + \sigma_{xx}^{\mathrm{QO}}(\mu)R_T R_W + \sigma_{xx}^{\mathrm{SO}}(\mu), \tag{63}$$

where $\overline{\sigma}_{xx}^{(0)}(\mu)$ represents the nonoscillating part of conductivity given by Eq. (35), $\sigma_{xx}^{\mathrm{QO}}(\mu)$ describes the MQO of intralayer conductivity given by Eq. (39), and $\sigma_{xx}^{\mathrm{SO}}(\mu)$ describes the slow oscillations of intralayer conductivity given by Eq. (45). The second term, representing MQO, acquires two damping factors R_T and R_W from temperature and macroscopic sample inhomogeneities.

The quantum oscillations of interlayer conductivity $\sigma_{zz}^{\mathrm{QO}}(\mu)$, instead of being given by Eq. (39), are given by Eq. (18) of Ref. [33], which can be rewritten as

$$\sigma_{zz}^{\mathrm{QO}}(\mu) \approx 2\overline{\sigma}_{zz}^{(0)}\cos(\overline{\alpha})R_D\left[J_0(\lambda) - \frac{2}{\lambda}(1+\gamma_0)J_1(\lambda)\right]. \tag{64}$$

Let us compare Eq. (39) for $\sigma_{xx}^{\mathrm{QO}}$ with Eq. (64) for $\sigma_{zz}^{\mathrm{QO}}$. They look similar but have several important differences.

(i) The total sign "−" is responsible for the phase shift π of MQO of in-plane σ_{xx} with respect to interlayer σ_{zz} conductivity.

(ii) The amplitude of MQO of σ_{xx}, given by Eq. (41), is nonzero even in the beat nodes.

(iii) The additional field-dependent phase shift of MQO of intralayer conductivity is given by Eq. (42).

(iv) The expression in the square brackets in Eq. (64), responsible for the amplitude oscillations (beats) of MQO of interlayer conductivity, contains extra term $\propto J_1(\lambda)$, which gives the field-dependent phase shift ϕ_b of beats of MQO of σ_{zz} [33,42].

This phase shift ϕ_b contains the parameter $2(1+\gamma_0)/\lambda = (1+\gamma_0)\hbar\omega_c/(2\pi t_z)$, which is not small in strongly anisotropic Q2D metals. This factor increases with the increase of magnetic field; it is ~ 1 in strongly anisotropic Q2D metals and $\ll 1$ in weakly anisotropic almost 3D metals. For the in-plane conductivity σ_{xx} in Eq. (39) a similar term results not in the phase shift of beats but in the phase shift of MQO themselves, given by Eq. (42). It is small by the parameter $\lambda/\overline{\alpha} = 2t_z/E_F$ and is approximately field independent. In strongly anisotropic Q2D metals $2t_z/E_F \ll 1$, and this phase shift is negligibly small. However, in weakly anisotropic Q2D metals this parameter $\lambda/\overline{\alpha} = 2t_z/E_F \sim 1$, although they have a cylindrical Fermi surface and are far from the Lifshitz transition and magnetic breakdown, i.e., $E_F - 2t_z \gg \hbar\omega_c$.

To measure the proposed phase shift of fast Shubnikov oscillations one can compare the phase of Shubnikov and de Haas–van Alphen oscillations. The latter are determined by the oscillations of the DOS [64,65]:

$$\rho(B_z) \approx \rho_0[1 - 2R_D J_0(\lambda)\cos(\overline{\alpha})], \tag{65}$$

where the nonoscillating part of the DOS (per one spin) is $\rho_0 = m_*/(2\pi\hbar^2 d)$, and the magnetization oscillations per one spin component are given by [33,65,66]

$$\widetilde{M}(B_z) \approx \frac{eE_F}{2\pi^2\hbar cd}R_D R_T\left[J_0(\lambda)\sin(\overline{\alpha}) + \frac{\lambda}{\overline{\alpha}}J_1(\lambda)\cos(\overline{\alpha})\right]. \tag{66}$$

Equations (65) and (66) are illustrated in Fig. 3 and compared to conductivity oscillations.

At low magnetic field, when $\lambda \gg 1$, the second term in the square brackets of Eq. (64) is small, and the MQO of σ_{zz} in Eq. (64) and of σ_{xx} in Eq. (39) are in antiphase. Note that the phase of σ_{xx} MQO coincides with the phase of DOS MQO given by Eq. (65). This is illustrated in Fig. 3. However, at high fields $\hbar\omega_c \gg 4\pi t_z$, expression (64) for interlayer conductivity $\sigma_{zz}^{\mathrm{QO}}$ asymptotically is equal to $-2\overline{\sigma}_{zz}^{(0)}\cos(\overline{\alpha})R_D[1+2\gamma_0]$, while $\sigma_{xx}^{\mathrm{QO}}$ is close to $-4\pi^2\overline{\sigma}_{xx}^{(0)}R_D\cos(\overline{\alpha})/(\gamma_0^2+\pi^2)$. Hence, at high magnetic fields the fast oscillations of σ_{xx}, σ_{zz}, and the DOS have the same phase. This agrees with the calculations of σ_{zz} within the two-layer model [30,31,53,67,68] and for 3D dispersion (4) at $\hbar\omega_c \gg t_z$ [52,54]. Hence, there is a crossover between these two regimes of σ_{zz} at $\lambda \sim 1$.

Let us now compare Eq. (45) for $\sigma_{xx}^{\mathrm{SO}}(\varepsilon)$ with the slow oscillations of interlayer conductivity $\sigma_{zz}^{\mathrm{SO}}(\varepsilon)$, given by Eqs. (18) or (19) of Ref. [33], which can be rewritten as

$$\sigma_{zz}^{\mathrm{SO}}(\mu) \approx 2\overline{\sigma}_{zz}^{(0)}R_D^2 J_0(\lambda)\left[J_0(\lambda) - \frac{2}{\lambda}J_1(\lambda)\right]. \tag{67}$$

Similar to the beats of fast MQO, the slow oscillations of interlayer conductivity σ_{zz} have a field-dependent phase shift

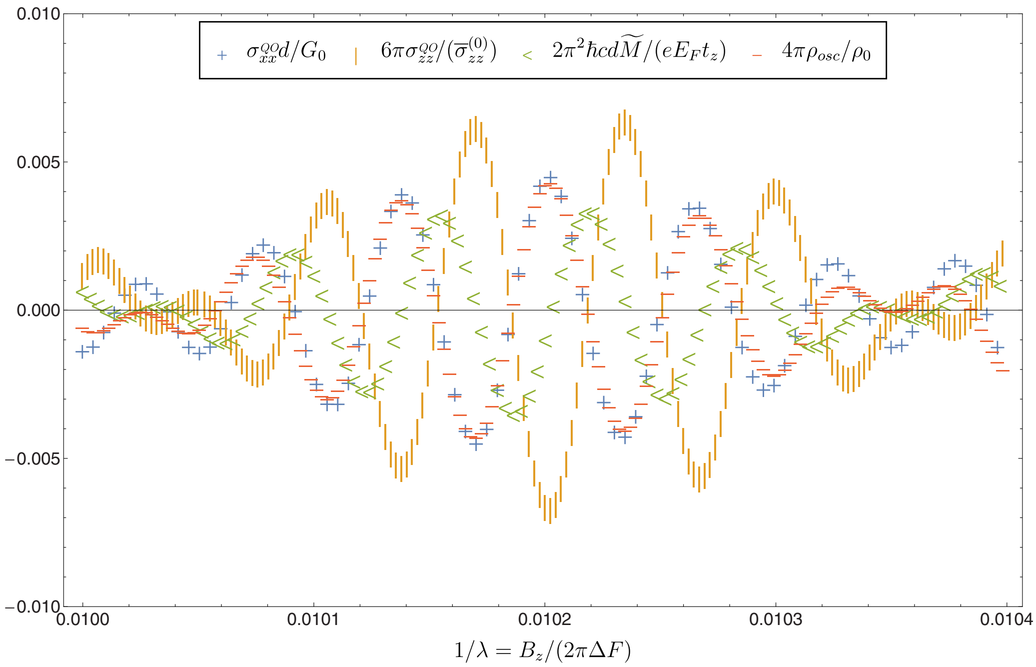

FIG. 3. Quantum oscillations of intralayer diagonal conductivity $\sigma_{xx}^{\rm QO}$, of interlayer conductivity $\sigma_{zz}^{\rm QO}$, and of magnetization $\widetilde{M}$ as a function $1/\lambda = B_z/(2\pi\Delta F)$. One can see that the oscillations of $\sigma_{zz}^{\rm QO}$ are shifted from $\widetilde{M}$ by a quarter of a period, but at $1/\lambda \approx 0.01036$ the phase shift is close to π. Except the beat nodes, the oscillations of σ_{xx} have the same phase as those of the density of states, but are in antiphase with the oscillations of σ_{zz}. The parameters for numerical calculations are $m_* = 0.04 m_e$, $\Gamma_0 = 14.5\,K$, $t_z = 10$ meV, $E_F = 200$ meV.

due to the second term $2J_1(\lambda)/\lambda$ in the square brackets of Eq. (67), which is absent in the SO of σ_{xx}. This phase shift $\phi_s^{zz} \sim 2/\lambda$ is small at $\lambda \gg 1$, i.e., everywhere except the last period of slow oscillations.

The main difference of the SO of interlayer $\sigma_{zz}^{\rm SO}$ and intralayer $\sigma_{xx}^{\rm SO}$ conductivity is that the amplitude of the latter depends nonmonotonically on $\gamma_0 = \pi/(\omega_c\tau_0)$, as one can see from Eq. (45): at $\gamma_0^2 = \pi^2/3$ the amplitude of SO of σ_{xx} changes sign, going through zero. At small $\gamma_0 < \pi/\sqrt{3}$, i.e., at large $\omega_c\tau_0 > \sqrt{3}$ when MQO are strong, the slow oscillations of intralayer σ_{xx} and interlayer σ_{zz} conductivity are in the same phase. At large $\gamma_0 > \pi/\sqrt{3}$, i.e., at small $\omega_c\tau_0 < \sqrt{3}$ when MQO are weak, the SO of σ_{xx} and σ_{zz} are in the antiphase. To demonstrate this phase shift π of SO of in-plane conductivity σ_{xx} with respect to interlayer conductivity σ_{zz}, in Fig. 4(a) we plot the amplitude

$$A_{xx}^{\rm SO} \equiv \frac{\pi}{2\lambda}\overline{\alpha}\gamma_0 R_D^2 \frac{\pi^2 - 3\gamma_0^2}{\left(\gamma_0^2 + \pi^2\right)^3} \tag{68}$$

of $\sigma_{xx}^{\rm SO} d/G_0$, where $G_0 = e^2/(\pi\hbar)$ is the quantum of conductance—the expression for the amplitude follows from the expression of $\sigma_{xx}^{\rm SO} d/G_0$ after using the asymptote of squared Bessel function $J_0^2(\lambda) \sim [1 + \sin(2\lambda)]/(\pi\lambda)$ for $\lambda \gg 1$ and extracting the coefficient before $\sin(2\lambda)$. In Fig. 4(b) we compare $\sigma_{xx}^{\rm SO} d/G_0$ given by Eq. (45) to $\sigma_{zz}^{\rm SO} d/G_0$ given by Eq. (67). Contrary to $\sigma_{xx}^{\rm SO}$, the amplitude of SO of interlayer conductivity $\sigma_{zz}^{\rm SO}$ in Eq. (67) monotonically decreases with increasing γ_0 (see Fig. 4). The nonmonotonic field dependence of the amplitude of slow oscillations of in-plane conductivity probably explains the π difference of the phase of SO of in-plane magnetoresistance observed [34] in rare-earth tritellurides $TbTe_3$ and $GdTe_3$ (see Fig. 6 of Ref. [34]).

V. SUMMARY

To summarize, we calculate the magnetic quantum oscillations of intralayer conductivity σ_{xx} in quasi-2D metals in quantizing magnetic field. This calculation is based on the Kubo formula and harmonic expansion. It takes into account the electron scattering by short-range impurities and neglects the electron-electron interaction. The latter approximation is justified in the metallic limit of a large number of filled LLs and finite interlayer transfer integral t_z. Previously, such calculation in quasi-2D metals was performed only for interlayer conductivity σ_{zz} [33,52]. We calculated analytically the amplitudes and phases of the usual MQO and the so-called slow oscillations with frequency $\propto t_z$, arising from the mixing of two close MQO frequencies. The SO appear only in the second order in the Dingle factor, but they are usually stronger than MQO, because the latter are additionally damped by temperature and sample inhomogeneities.

The comparison of the results for intralayer σ_{xx} and interlayer σ_{zz} conductivity shows several qualitative differences between their oscillations, discussed and illustrated above. The amplitude of SO of σ_{xx}, given by Eqs. (45) and (68) and illustrated in Fig. 4, has a nonmonotonic dependence on magnetic field. This amplitude changes sign at $\gamma_0 = \pi/(\omega_c\tau_0) = \pi/\sqrt{3}$, while the amplitude of SO of σ_{zz} is a monotonic function of field. The SO of σ_{xx} and σ_{zz} have opposite phase in weak magnetic field and same phase in strong field. The MQO of σ_{zz} have a crossover with a phase inversion at $\lambda \sim 1$, while MQO of σ_{xx} do not have such crossover. Therefore, similarly

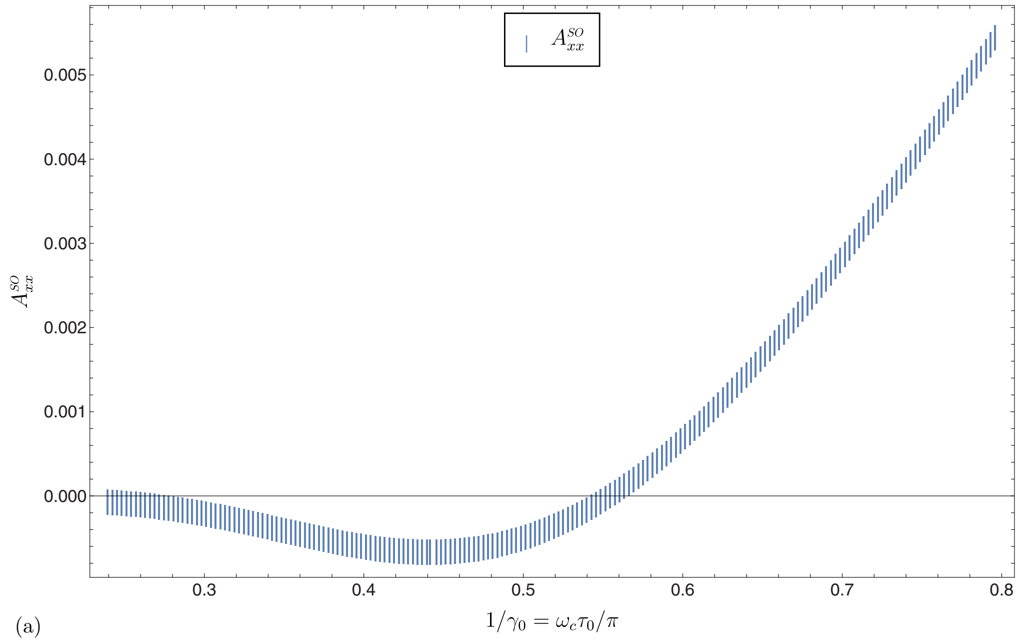

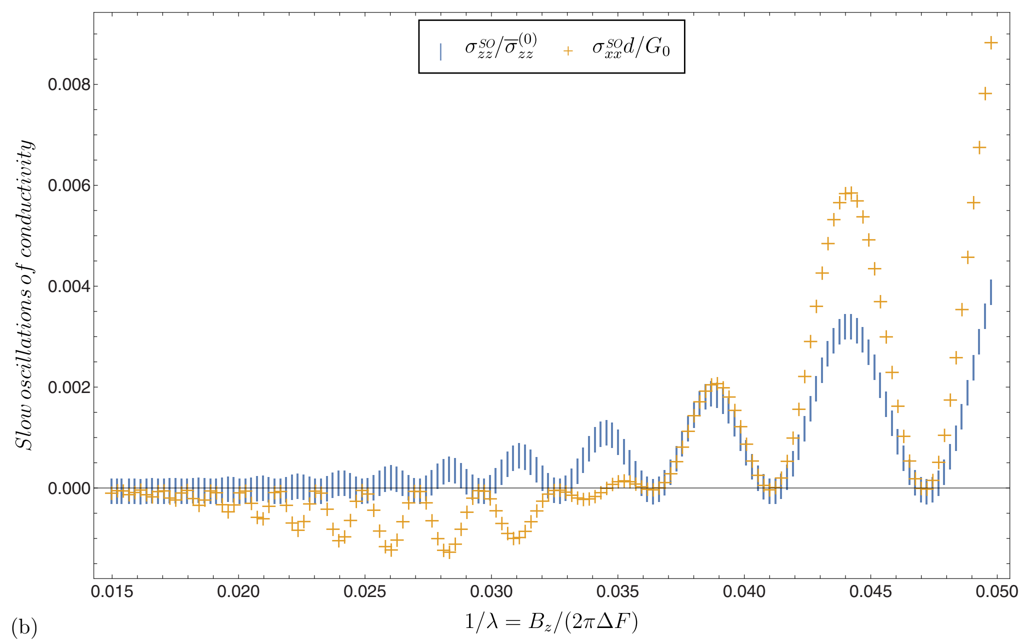

FIG. 4. The amplitude (a) and magnitude (b) of slow oscillations of σ_{xx} and σ_{zz}. The parameters are the same as in Fig. 3. (a) Amplitude A_{xx}^{SO} of slow oscillations of normalized intralayer diagonal conductivity $\sigma_{xx}^{\mathrm{SO}}d/G_0$ as a function of $1/\gamma_0 = \hbar\omega_c/(2\pi\Gamma_0) \propto B_z$. This plot demonstrates that the amplitude A_{xx}^{SO} changes its sign at $\gamma_0 = \pi/\sqrt{3}$. (b) Slow oscillations of intralayer σ_{xx} and interlayer σ_{zz} conductivity as a function of $1/\lambda = \hbar\omega_c/(4\pi t_z) \propto B_z$. The slow oscillations of σ_{xx} and σ_{zz} are in antiphase at low magnetic field and have the same phase at high field.

to SO, the MQO of σ_{zz} and σ_{xx} have opposite phase in weak magnetic field and same phase in strong field. This crossover between high- and low-field limits for MQO of σ_{zz} is driven by the parameter $\lambda = 4\pi t_z/(\hbar\omega_c)$, while for SO of σ_{xx} the driving parameter is $\gamma = 2\pi\Gamma/(\hbar\omega_c)$.

Notably, the oscillations of MQO amplitudes, called beats and arising from the interference of two close frequencies, for σ_{xx} are not complete, i.e., the amplitude of σ_{xx} oscillations is nonzero even in the beat nodes, as given by Eq. (41) and illustrated in Fig. 1. The field-dependent phase shift of beats, known for σ_{zz} MQO [33,42], does not appear in σ_{xx}. However, for σ_{xx} the phase of MQO themselves is shifted by the value $\sim t_z/E_F$, as given by Eqs. (39) and (42).

The developed theory and the results obtained are applicable to describe transverse magnetoresistance in various anisotropic quasi-2D conductors, including organic metals, high-T_c superconducting materials, heterostructures, intercalated graphite, rare-earth tritellurides, etc.

ACKNOWLEDGMENTS

The authors thank the senior scientist Pavel Streda from Department of Semiconductors of Institute of Physics of the Czech Academy of Sciences for the detailed explanation of his calculations. T.I.M. thanks Konstantin Nesterov and Pavel Nagornykh for stylistic corrections. The work was partially supported by the "BASIS" Foundation for the Development of Theoretical Physics. T.I.M. acknowledges Russian Foundation for Basic Research Grants No. 18-32-00205, No. 18-02-01022, and No. 18-02-00280. P.D.G. acknowledges Program No. 0033-2018-0001: "Condensed Matter Physics."

[1] A. A. Abrikosov, *Fundamentals of the Theory of Metals* (North-Holland, Amsterdam, 1988).

[2] J. M. Ziman, *Principles of the Theory of Solids* (Cambridge University, Cambridge, England, 1972).

[3] D. Shoenberg, *Magnetic Oscillations in Metals* (Cambridge University, Cambridge, England, 1984).

[4] M. V. Kartsovnik, Chem. Rev. **104**, 5737 (2004).

[5] J. Singleton, Rep. Prog. Phys. **63**, 1111 (2000).

[6] T. Ishiguro, K. Yamaji, and G. Saito, *Organic Superconductors*, 2nd ed. (Springer-Verlag, Berlin, 1998).

[7] M. V. Kartsovnik and V. G. Peschansky, Low Temp. Phys. **31**, 185 (2005) [Fiz. Nizk. Temp. **31**, 249 (2005)].

[8] J. Wosnitza, *Fermi Surfaces of Low-Dimensional Organic Metals and Superconductors* (Springer-Verlag, Berlin, Heidelberg, 1996).

[9] *The Physics of Organic Superconductors and Conductors*, edited by A. G. Lebed (Springer-Verlag, Berlin, 2008).

[10] N. E. Hussey, M. Abdel-Jawad, A. Carrington, A. P. Mackenzie, and L. Balicas, Nature (London) **425**, 814 (2003).

[11] N. Doiron-Leyraud, C. Proust, D. LeBoeuf, J. Levallois, J. B. Bonnemaison, R. Liang, D. A. Bonn, W. N. Hardy, and L. Taillefer, Nature (London) **447**, 565 (2007).

[12] S. E. Sebastian, N. Harrison, E. Palm, T. P. Murphy, C. H. Mielke, R. Liang, D. A. Bonn, W. N. Hardy, and G. G. Lonzarich, Nature (London) **454**, 200 (2008).

[13] A. Audouard, C. Jaudet, D. Vignolles, R. Liang, D. A. Bonn, W. N. Hardy, L. Taillefer, and C. Proust, Phys. Rev. Lett. **103**, 157003 (2009).

[14] J. Singleton, C. de la Cruz, R. D. McDonald, S. Li, M. Altarawneh, P. Goddard, I. Franke, D. Rickel, C. H. Mielke, Xin Yao, and P. Dai, Phys. Rev. Lett. **104**, 086403 (2010).

[15] S. E. Sebastian, N. Harrison, M. M. Altarawneh, C. H. Mielke, R. Liang, D. A. Bonn, W. N. Hardy, and G. G. Lonzarich, Proc. Natl. Acad. Sci. USA **107**, 6175 (2010).

[16] S. E. Sebastian, N. Harrison, P. A. Goddard, M. M. Altarawneh, C. H. Mielke, R. Liang, D. A. Bonn, W. N. Hardy, O. K. Andersen, and G. G. Lonzarich, Phys. Rev. B **81**, 214524 (2010).

[17] S. E. Sebastian, N. Harrison, R. Liang, D. A. Bonn, W. N. Hardy, C. H. Mielke, and G. G. Lonzarich, Phys. Rev. Lett. **108**, 196403 (2012).

[18] S. E. Sebastian, N. Harrison, F. F. Balakirev, M. M. Altarawneh, P. A. Goddard, R. Liang, D. A. Bonn, W. N. Hardy, and G. G. Lonzarich, Nature (London) **511**, 61 (2014).

[19] N. Doiron-Leyraud, S. Badoux, S. Rene de Cotret, S. Lepault, D. LeBoeuf, F. Laliberte, E. Hassinger, B. J. Ramshaw, D. A. Bonn, W. N. Hardy, R. Liang, J. H. Park, D. Vignolles, B. Vignolle, L. Taillefer, and C. Proust, Nat. Commun. **6**, 6034 (2015).

[20] S. E. Sebastian, N. Harrison, and G. G. Lonzarich, Rep. Prog. Phys. **75**, 102501 (2012).

[21] B. Vignolle, D. Vignolles, M. H. Julien, and C. Proust, C. R. Phys. **14**, 39 (2013).

[22] S. E. Sebastian and C. Proust, Annu. Rev. Condens. Matter Phys. **6**, 411 (2015) and references therein.

[23] T. Ando, A. B. Fowler, and F. Stern, Rev. Mod. Phys. **54**, 437 (1982).

[24] B. Huckestein, Rev. Mod. Phys. **67**, 357 (1995).

[25] K. Yamaji, J. Phys. Soc. Jpn. **58**, 1520 (1989).

[26] M. V. Kartsovnik, P. A. Kononovich, V. N. Laukhin, and I. F. Shchegolev, Pis'ma Zh. Eksp. Teor. Fiz. **48**, 498 (1988) [JETP Lett. **48**, 541 (1988)].

[27] R. Yagi, Y. Iye, T. Osada, and S. Kagoshima, J. Phys. Soc. Jpn. **59**, 3069 (1990).

[28] Y. Kurihara, J. Phys. Soc. Jpn. **61**, 975 (1992).

[29] P. Moses and R. H. McKenzie, Phys. Rev. B **60**, 7998 (1999).

[30] P. D. Grigoriev and T. I. Mogilyuk, Phys. Rev. B **90**, 115138 (2014).

[31] P. D. Grigoriev and T. I. Mogilyuk, Phys. Rev. B **95**, 195130 (2017).

[32] M. V. Kartsovnik, P. D. Grigoriev, W. Biberacher, N. D. Kushch, and P. Wyder, Phys. Rev. Lett. **89**, 126802 (2002).

[33] P. D. Grigoriev, Phys. Rev. B **67**, 144401 (2003).

[34] P. D. Grigoriev, A. A. Sinchenko, P. Lejay, A. Hadj-Azzem, J. Balay, O. Leynaud, V. N. Zverev, and P. Monceau, Eur. Phys. J. B **89**, 151 (2016).

[35] M. V. Kartsovnik, V. N. Laukhin, V. I. Nizhankovskii, and A. Ignat'ev, Pis'ma Zh. Eksp. Teor. Fiz. **47**, 302 (1988) [JETP Lett. **47**, 363 (1988)].

[36] M. V. Kartsovnik, P. A. Kononovich, V. N. Laukhin, S. I. Pesotskii, and I. F. Schegolev, Pis'ma Zh. Eksp. Teor. Fiz. **49**, 453 (1989) [JETP Lett. **49**, 519 (1989)].

[37] J. Wosnitza, D. Beckmann, G. Goll, and D. Schweitzer, Synth. Metals **85**, 1479 (1997).

[38] E. Ohmichi, H. Ito, T. Ishiguro, G. Saito, and T. Komatsu, Phys. Rev. B **57**, 7481 (1998).

[39] B. Narymbetov, N. Kushch, L. Zorina, S. Khasanov, R. Shibaeva, T. Togonidze, A. Kovalev, M. Kartsovnik, L. Buravov, E. Yagubskii, E. Canadell, A. Kobayashi, and H. Kobayashi, Eur. Phys. J. B **5**, 179 (1998); T. Togonidze, M. Kartsovnik, J. Perenboom, N. Kushch, and H. Kobayashi, Physica B **294**, 435 (2001).

[40] P. D. Grigoriev and T. Ziman, JETP Lett. **106**, 371 (2017).

[41] P. D. Grigoriev and T. Ziman, Phys. Rev. B **96**, 165110 (2017).

[42] P. D. Grigoriev, M. V. Kartsovnik, W. Biberacher, N. D. Kushch, and P. Wyder, Phys. Rev. B **65**, 060403(R) (2002).

[43] P. D. Grigoriev, M. M. Korshunov, and T. I. Mogilyuk, J. Supercond. Nov. Magn. **29**, 1127 (2016).

[44] The case $t_z(\boldsymbol{k}_\parallel) \neq \text{const}$ was also studied [45–47].
[45] C. Bergemann, S. R. Julian, A. P. Mackenzie, S. NishiZaki, and Y. Maeno, Phys. Rev. Lett. **84**, 2662 (2000).
[46] P. D. Grigoriev, Phys. Rev. B **81**, 205122 (2010).
[47] M. V. Kartsovnik, V. N. Laukhin, S. I. Pesotskii, I. F. Schegolev, and V. M. Yakovenko, J. Phys. I (France) **2**, 89 (1992).
[48] E. N. Economou, *Green's Functions in Quantum Physics*, 3rd ed. (Springer-Verlag, Berlin, 2006).
[49] A. A. Abrikosov, L. P. Gor'kov, and I. E. Dzyaloshinski, *Methods of Quantum Field Theory in Statistical Physics* (Dover, New York, 1975).
[50] P. Streda and L. Smrcka, Phys. Status Solidi B **70**, 537 (1975).
[51] A. Bastin, C. Lewiner, O. Betbeder-matibet, and P. Nozieres, J. Phys. Chem. Solids **32**, 1811 (1971).
[52] T. Champel and V. P. Mineev, Phys. Rev. B **66**, 195111 (2002).
[53] P. D. Grigoriev, Phys. Rev. B **83**, 245129 (2011).
[54] P. D. Grigoriev, Phys. Rev. B **88**, 054415 (2013).
[55] This property for the scattering by pointlike impurities can be proved even in the "noncrossing" approximation [53].
[56] J. R. Wilton, J. Lond. Math. Soc. **s1-5**, 276 (1930).
[57] I. S. Gradshteyn and I. M. Ryzhik, *Table of Integrals, Series, and Products* (Academic, New York, 1980).
[58] A. P. Prudnikov, Yu. A. Brychkov, and O. I. Marichev, *Integrals and Series* (Gordon and Breach, New York, 1990), Vol. 2.
[59] In fast quantum oscillations we keep only the first-order term in the Dingle factor. However, in slow oscillations we keep also the second-order terms, because contrary to fast quantum oscillations they are not damped by temperature and sample inhomogeneities.
[60] T. Ando, J. Phys. Soc. Jpn. **37**, 1233 (1974).
[61] I. M. Lifshitz and L. M. Kosevich, Zh. Eksp. Teor. Fiz. **33**, 88 (1957) [Sov. Phys. JETP **6**, 67 (1958)].
[62] E. M. Lifshitz and L. P. Pitaevsky, *Physical Kinetics* (Pergamon, Oxford, 1981).
[63] After Eq. (90.22) of Ref. [62] it is mistakenly written "+" for maximum and "−" for minimum, which differs from the sign in the original paper [61] and in our calculations.
[64] T. Champel and V. P. Mineev, Philos. Mag. B **81**, 55 (2001).
[65] P. D. Grigoriev, J. Exp. Theor. Phys. **92**, 1090 (2001).
[66] T. Champel, Phys. Rev. B **64**, 054407 (2001).
[67] P. D. Grigoriev, M. V. Kartsovnik, and W. Biberacher, Phys. Rev. B **86**, 165125 (2012).
[68] A. D. Grigoriev and P. D. Grigoriev, Low Temp. Phys. **40**, 367 (2014).